



PCCP

**In silico discovery of active, stable, CO-tolerant and cost-effective electrocatalysts for hydrogen evolution and oxidation**

Journal:	<i>Physical Chemistry Chemical Physics</i>
Manuscript ID	CP-COM-06-2020-003017.R1
Article Type:	Communication
Date Submitted by the Author:	31-Jul-2020
Complete List of Authors:	Back, Seoin; Sogang University, Chemical and Biomolecular Engineering Na, Jonggeol; Ewha Womans University, Division of Chemical Engineering and Materials Science Tran, Kevin; Carnegie Mellon University, Chemical Engineering Ulissi, Zachary; Carnegie Mellon University, Chemical Engineering

SCHOLARONE™  
Manuscripts

Cite this: DOI: 00.0000/xxxxxxxxxx

## In silico discovery of active, stable, CO-tolerant and cost-effective electrocatalysts for hydrogen evolution and oxidation

Seoin Back,<sup>a,‡\*</sup> Jonggeol Na,<sup>b,‡</sup> Kevin Tran,<sup>c</sup> and Zachary W. Ulissi<sup>c\*</sup>

Received Date

Accepted Date

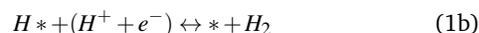
DOI: 00.0000/xxxxxxxxxx

Various databases of density functional theory (DFT) calculations for materials and adsorption properties are currently available. Using Materials Project and GAspy database of materials stability and binding energies ( $H^*$  and  $CO^*$ ), respectively, we evaluate multiple aspects of catalysts to discover active, stable, CO-tolerant, and cost-effective hydrogen evolution and oxidation catalysts. Finally, we suggest a few candidate materials for future experimental validations. We highlight that the stability analysis is easily obtainable but provides invaluable information to assess thermodynamic and electrochemical stability, bridging the gap between simulations and experiments. Further, it reduces the number of expensive DFT calculations required to predict catalytic activities of surfaces by filtering out unstable materials.

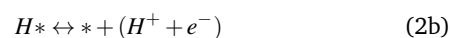
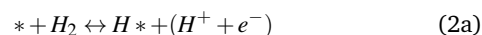
Hydrogen evolution reaction (HER, Eqn. (1a) and (1b)) and oxidation reaction (HOR, Eqn. (2a) and (2b)) are key reactions in future energy technologies as a cathodic half-cell reaction in water electrolyzer and an anodic half-cell reaction in the fuel cell, respectively.<sup>1</sup> Pt group metal catalysts are known to be the best for both reactions with very small overpotentials and high stability in acidic conditions.<sup>2</sup> However, scarcity and high cost of Pt group metals have held back their widespread use, and it has triggered significant research efforts to develop non-Pt group metal catalysts with activity and stability comparable to Pt. Various non-Pt group catalysts have shown a reasonable activity for HER/HOR in alkaline conditions, but their performances in acid have barely been reported probably because they are unstable in acidic conditions against an oxidation or a dissolution.<sup>3–6</sup> Although the kinetics of HER and HOR are facile in both acidic and

alkaline conditions, a discovery of acid-stable catalysts is significantly preferred, since acidic oxygen reduction reaction (ORR) and evolution reaction (OER), the other half-cell reactions in the fuel cell and water electrolyzer, respectively, have several advantages over alkaline conditions such as high current densities and lower Ohmic loss.<sup>7–9</sup>

Hydrogen Evolution Reaction (HER)



Hydrogen Oxidation Reaction (HOR)



HER and HOR are two proton-electron transfer reactions with only one reaction intermediate involved ( $H^*$ , where "\*" indicates an adsorbed reaction intermediate on the catalyst surface), and one reaction is a reverse reaction of the other. Note that expressions for reactions could be different in the alkaline condition as  $H_2O$  acts as a proton donor instead of  $H^+$  in the acidic condition. In this case, we can use the following relation:  $H_2O(l) \leftrightarrow H^+(aq) + OH^-(aq)$ , which is in equilibrium at neutral pH, with additional correction terms for pH ( $\Delta G_{H^+}(pH)$ ). As the correction term is added to both sub-reactions of HER and HOR, the pH effect essentially does not affect the overall catalytic activity in this scheme. Using a binding free energy of the reaction intermediate ( $\Delta G_{H^*}$ ) as an activity descriptor, density functional theory (DFT) calculations have shown a great correlation with experimentally measured current densities,<sup>10</sup> and it has been a basis for high-throughput screening to discover new materials.<sup>11</sup> In the last decade, various materials such as metal alloys and metal-doped two-dimensional materials have been computationally modeled, and their catalytic activities for HER/HOR have been evaluated on the basis of  $\Delta G_{H^*}$  to calculate the thermodynamic overpotentials ( $\eta_{HER/HOR}$ ).<sup>12–15</sup> However, we note that electrochemical stability

<sup>a</sup> Department of Chemical and Biomolecular Engineering, Sogang University, Seoul 04107, Republic of Korea; E-mail: sback@sogang.ac.kr

<sup>b</sup> Division of Chemical Engineering and Materials Science, Ewha Womans University, Seoul 03760, Republic of Korea;

<sup>c</sup> Department of Chemical Engineering, Carnegie Mellon University, Pittsburgh, PA, USA; E-mail: zulissi@andrew.cmu.edu

† Electronic Supplementary Information (ESI) available: [Computational details and promising candidates identified]. See DOI: 00.0000/00000000.

‡ These authors contributed equally to this work.

of catalysts under HER/HOR conditions has been barely considered, although it is a key factor to evaluate the potential of catalysts particularly under the acidic environment. Recently, Jain et al. highlighted the importance of considering the electrochemical stability under the harsh oxygen reduction and evolution reaction conditions when evaluating the potential of new promising materials.<sup>16</sup> Further, CO tolerance has also barely been evaluated simultaneously, though it could significantly affect the number of active sites on the surface.

In this work, we present *in silico* discovery of active, stable, CO-tolerant, and cost-effective HER/HOR catalysts. We evaluated multiple aspects of catalysts using DFT database of stability and binding energy. To obtain massive data on stability and binding energy ( $H^*$  and  $CO^*$ ), we employed Materials Project<sup>17</sup> and GASpy database<sup>18</sup>, respectively. We note that GASpy database contains  $CO^*$  and  $H^*$  binding energies on intermetallic alloy surfaces with all unique active sites of multiple facets considered (see Supporting Information for more details). Considering all these factors, we present a list of promising candidate materials for HER/HOR under acidic conditions. Multiple aspects were considered to evaluate the potential of catalysts: (1) electrochemical activity, (2) thermodynamic stability, (3) electrochemical stability, (4) CO tolerance and (5) price. In the following, we present how each aspect was evaluated in detail.

### Electrochemical activity

We assessed HER/HOR catalytic activities based on the theoretical overpotentials using the computational hydrogen electrode (CHE) method,<sup>19</sup> where the chemical potential of a proton-electron pair is assumed to be equal to a half of that of gas-phase  $H_2$  in standard conditions, *i.e.*,  $G(H^+ + e^-) = \frac{1}{2}G(H_2)$ . It enables to calculate H binding free energy ( $\Delta G_{H^*}$ ) from the first reaction step of HER (Eqn (1a)). Since the adsorbed H is the only intermediate for both HER and HOR, the theoretical overpotentials ( $\eta$ ) for HER and HOR are identical and calculated as Eqn (3). Recently, Lindgre *et al.* suggested Pt being the ideal catalyst for the HER because the surface active sites, *i.e.*, typically the strongest binding hollow sites, are already fully covered via underpotential deposition (UPD), and less strongly bound  $H^*$  at top sites contributes to energetically favorable association reaction (Tafel step) through coupling between  $H^*$  at the top sites, compared to the coupling between  $H^*$  at the hollow sites.<sup>20</sup> This observation suggests that  $\Delta G_{H^*} \sim 0$  eV as in the case of Pt (111) is a necessary condition to be the optimal HER catalysts. According to this observation, we decided to consider only the most stable and top site binding to allow facile  $H^*-H^*$  coupling. Out of 23,050 DFT calculated data for H adsorption from GASpy database<sup>18</sup> (see Supplementary Information for more details), we collected the most stable binding energies on each surface (4,993 data), considered catalyst surfaces that are predicted to have  $\eta_{HER/HOR} \leq 0.2$  V (1,555 data), and collected the top-site binding configurations (573 data).

$$\eta_{HER/HOR} (V) = \frac{|\Delta G_{H^*}|}{e} \quad (3)$$

### Thermodynamic stability

We evaluated the thermodynamic stability based on energy above hull, which is the distance from the convex hull of each combination in phase diagrams. The phase diagram is generated by plotting formation energies of all possible combinations of consisting elements in Materials Project database and the convex hull is constructed by connecting the most stable phases at each composition.<sup>17</sup> Thus, the energy above hull represents the relative stability of materials with respect to the most stable phase at that composition. More positive values of the energy above hull indicate stronger driving forces to decompose into the most stable compounds of the element combinations. We note that the phase diagram and the energy above hull are approximations based on the existing materials in Materials Project, and the complete exploration of continuous compositions of the combinations could affect the results. We assume materials with the energy above hull smaller than 0.05 eV to be stable.

### Electrochemical stability

In addition to the energy above hull, which considers the relative stability of alloys with various compositions, one needs to further evaluate the stability with respect to ions and oxides at reaction conditions (pH and potential). This is because metals could undergo a dissolution or oxidation during the reaction. Persson et al. reported an approach to predict solid-aqueous equilibria and to generate the Pourbaix diagram by combining first-principles calculations of solids and experimental data of aqueous species<sup>21</sup>, which is now implemented in Materials Project<sup>17</sup>. We used this approach to calculate the electrochemical stability ( $\Delta G_{Pourbaix}$ ) of bulk structures relative to the most stable phases at 0.2 V of  $\eta_{HER/HOR}$ , *i.e.*,  $-0.2$  and  $+0.2$   $V_{RHE}$  for HER and HOR, respectively. pH=0 was set to evaluate the stability under the acidic condition. The results for neutral (pH=7) and alkaline (pH=14) conditions are available in the Github. We note that the Pourbaix diagram is constructed based only on thermodynamic data. Thus it cannot evaluate the kinetic stability of the dissolution or the oxidation. For example, if catalysts are thermodynamically unstable but the dissolution or the oxidation is kinetically sluggish, we could expect a few hours of stability.<sup>22</sup> Further, it only considers the stability of bulk phases. Thus surface stabilities cannot be evaluated based on this approach. However,  $\Delta G_{Pourbaix}$  could at least be used as a lower limit to filter out unstable bulk materials.<sup>16</sup>

### CO tolerance

It has been observed that Pt catalysts severely suffer from carbon monoxide (CO) poisoning even when traces amount of CO present in the fuel gas of the fuel cell, resulting in a degradation of the performance.<sup>23</sup> Strong CO adsorption reduces the number of surface active sites available, and the pre-occupied CO could even change energetics of H adsorptions originated from the coverage effect, thus affecting the catalytic activities<sup>24</sup>. We assumed catalyst surfaces with  $\Delta G_{CO^*}$  weaker (more positive) than  $-0.2$  eV free from the CO poisoning, considering 0.2 eV of the DFT uncertainty compared to the experiments.<sup>25,26</sup> We found that

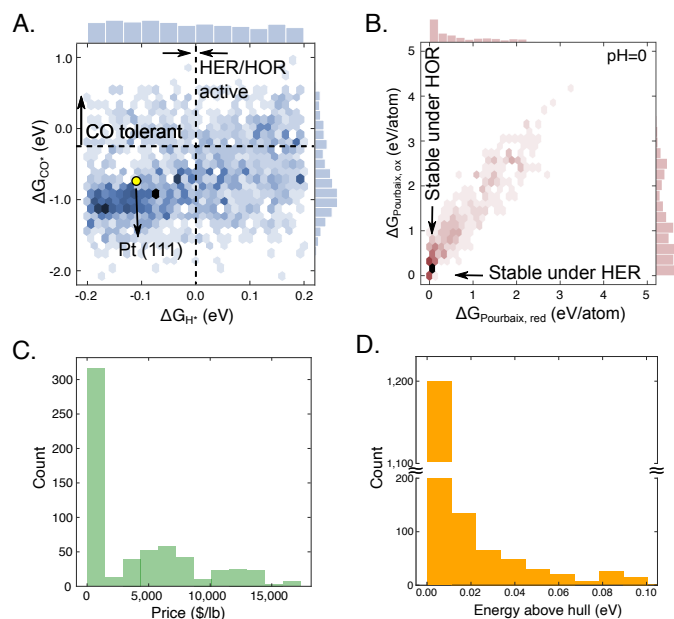


Fig. 1 Two-dimensional histograms of (A)  $\Delta G_{H^*}$  and  $\Delta G_{CO^*}$  and (B) electrochemical stability ( $\Delta G_{Pourbaix}$ ) at reduction ( $-0.2 V_{RHE}$ ) and oxidation conditions ( $+0.2 V_{RHE}$ ) at pH=0. Histograms of (C) prices and (D) energy above hull.

$\Delta G_{CO^*}$  is unavailable for some surfaces in GASpy database. For those surfaces, we predicted  $\Delta G_{CO^*}$  using regression models developed based on  $\sim 20,000$  DFT calculations with the prediction accuracy of 0.20 eV of mean absolute error for test set.<sup>18</sup> The regression model is based on active site-related fingerprints including atomic radii, Pauling electronegativity, coordination number of the binding sites and median  $CO^*$  binding energy of the coordinating atoms. Using these fingerprints, the optimal regression method was searched using an automated machine learning package, TPOT<sup>27</sup>.

### Price

We collected element prices from "minerals.usgs.gov" and estimated prices of materials as follows:

$$Price (\$/lbs) = \frac{(P_A \times n_A \times m_A + P_B \times n_B \times m_B)}{(n_A \times m_A + n_B \times m_B)} \quad (5)$$

where  $P$  and  $n$  correspond to the element price, and the number of each element in the formula unit of the materials, respectively, and  $m$  is an atomic mass taken from the IUPAC technical report<sup>28</sup>, implemented in ASE<sup>29</sup>. We note that the calculated prices could be different from the ones required in the actual experiments since different reagents are used for different target materials. However, we expect the trend of alloy prices calculated based on the element prices be maintained because of a clear separation between inexpensive and expensive elements (Figure S1). The element prices are summarized in Table S1.

### Analysis

Figure 1 summarizes the results of our analysis on five aspects. As mentioned above, Figure 1A only shows the catalyst surfaces with

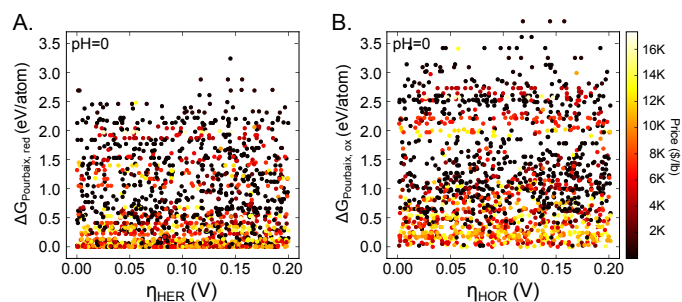


Fig. 2 The calculated electrochemical stabilities at pH=0 are plotted versus (a) HER and (b) HOR overpotentials.  $\Delta G_{Pourbaix}$  were calculated at  $-0.2 V_{RHE}$  and  $+0.2 V_{RHE}$  for HER and HOR, respectively. Catalysts positioned more to the left and the bottom indicate higher catalytic activity and stability under the reaction conditions, respectively. Marker colors correspond to their prices.

$\eta_{HER/HOR} \leq 0.2$  V. As a reference,  $\eta$  of the most active Pt catalysts were 0.11 V and 0.28 V, and  $\Delta G_{CO^*}$  were  $-0.87$  eV and  $-1.30$  eV for Pt (111) and Pt (211), respectively. In Figure 1A, a majority of catalyst surfaces bind CO very strongly, as highlighted by the high population at  $\Delta G_{CO^*} \sim -1.0$  eV. We note that the scaling relation between  $\Delta G_{CO^*}$  and  $\Delta G_{H^*}$  was not observed, while the strong correlation was observed for pure metal surfaces.<sup>30</sup> This difference may be originated from a chemical space we explored, consisting of much larger collections of surface compositions and structures compared to the simple monometallic systems with the limited variations of crystal structures and surfaces. We explicitly compared in our previous study<sup>31</sup> how our dataset is different from the conventional ones. Figure 1B predicts the electrochemical stability at pH=0 representing the acidic condition. We highlight that the electrochemical stability of catalysts is simple to obtain from Materials Project, but very useful, which has barely been investigated in the high-throughput screening of catalysts<sup>16</sup>. We observed a linear correlation between the stability under the reduction ( $-0.2 V_{RHE}$ ) and the oxidation ( $+0.2 V_{RHE}$ ) conditions, probably due to the close potential gap (0.4 V) between two conditions. It is noteworthy that there are high populations near the origin of the plots, indicating many catalysts could survive even at the acidic HER/HOR conditions. Figure 1C and D show histograms of price and energy above hull, where low prices and energy above hull close to 0 eV are preferred.

In Figure 2, we plotted the most important three factors simultaneously, electrochemical activity ( $\eta_{HER/HOR}$ ), electrochemical stability and price. Consistent with the common knowledge, many materials consisting of expensive noble metals are predicted to be stable at both conditions, evidenced by the high population of expensive materials near  $\Delta G_{Pourbaix}$  of 0 eV/atom. Note that materials are generally less stable at  $+0.2 V_{RHE}$  compared to  $-0.2 V_{RHE}$  as also shown in Figure 1B as a positive bias in the linear relation. This is because the high potential more strongly drives the oxidation, making materials relatively less stable. This is more noticeable for inexpensive materials, where only a few materials remained to be stable at the HOR condition.

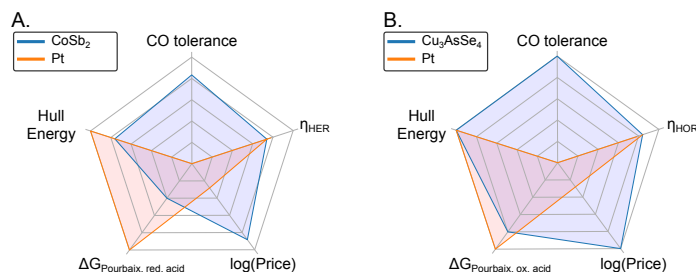


Fig. 3 Examples of the promising candidates for acid-stable (A) HER ( $\text{CoSb}_2$ ) and (B) HOR ( $\text{Cu}_3\text{AsSe}_4$ ) and their properties plotted in radar charts. Closer to the angular points correspond to better target properties. Scales are arbitrarily set based on the relative magnitudes of each property of two materials. Properties of Pt (111) are shown for comparison.

### Promising Candidates

We evaluated all five aspects of materials sequentially (denoted as "linear filtering") to suggest the promising candidates for acidic HER and HOR. A full list of the summarized data is available in the Github. For 23,050 DFT calculations of H adsorptions, we collected the most stable H adsorption energies for each surface and filtered out catalyst surfaces with  $\eta_{\text{HER/HOR}} > 0.2$  V, which reduced the number of surfaces to 1,555. Among 1,555 surfaces, we only adopted the top site binding for facile kinetics<sup>20</sup>, resulting in 573 surfaces. We then collected materials with  $\Delta G_{\text{Pourbaix}} < 0.1$  eV/atom at acidic conditions to ensure the electrochemical stability, resulting in 134 and 14 data, respectively. The number of acid stable materials at the HER condition is a lot more compared to the HOR condition as discussed in Figure 2. The criteria for the hull energy was set to 0.05 eV, which removed 5 and 1 materials. We then removed the surfaces with  $\Delta G_{\text{CO}^*} < -0.2$  eV and obtained 22 and 5 surfaces. Among these surfaces, 6 and 4 surfaces are based on cost-effective materials, cheaper than 100 \$/lb.

In Figure 3, we present the most promising candidates for active, stable, CO tolerant, and cost-effective HER and HOR catalysis found from the linear filtering,  $\text{CoSb}_2$  and  $\text{Cu}_3\text{AsSe}_4$ , respectively. The calculated HER/HOR overpotentials of promising catalysts are similar to that of Pt with the top-site binding to achieve facile kinetics, and their CO tolerance and price are extraordinarily superior to the Pt catalysts. The electrochemical stability (0.06 eV/atom vs. 0.00 eV/atom for Pt) and energy above hull (0.012 eV vs. 0.00 eV/atom for Pt) properties of  $\text{CoSb}_2$  are slightly worse compared to the Pt catalysts, while  $\text{Cu}_3\text{AsSe}_4$  showed excellent properties in all aspects. The detailed data on the electrochemical stability and the catalytic activity of the promising candidates are summarized in Figure S3 and S4, respectively.

The above linear filtering is significantly weighted with respect to the electrochemical stability since all materials with  $\Delta G_{\text{Pourbaix}} > 0.1$  eV/atom were filtered out at the first step. Additionally, we performed the Pareto optimal filtering analysis with visualization of data on two-dimensional latent space using t-distributed stochastic neighbor embedding (t-SNE<sup>32</sup>) to find candidates, and compared with the candidates found from the linear filtering (Figure 4). In the Pareto optimal filtering, we equally weighted four

properties ( $\eta_{\text{HER/HOR}}$ , CO tolerance,  $\Delta G_{\text{Pourbaix}}$  and hull energy). 19 and 20 Pareto optimal filtered surfaces for HER and HOR catalysts are obtained, respectively, and full candidates are listed in Table S4 and S5. Although some of Pareto and linear filtered candidates are located closely on the latent space, they were not exactly the same. As expected, the electrochemical stability of candidates suggested by the linear filtering is found to be better than those suggested by the Pareto filtering. On the other hand, other properties ( $\eta_{\text{HER/HOR}}$ , CO tolerance, and Hull energy) were found to be much better in the case of the Pareto filtering (Figure S1).

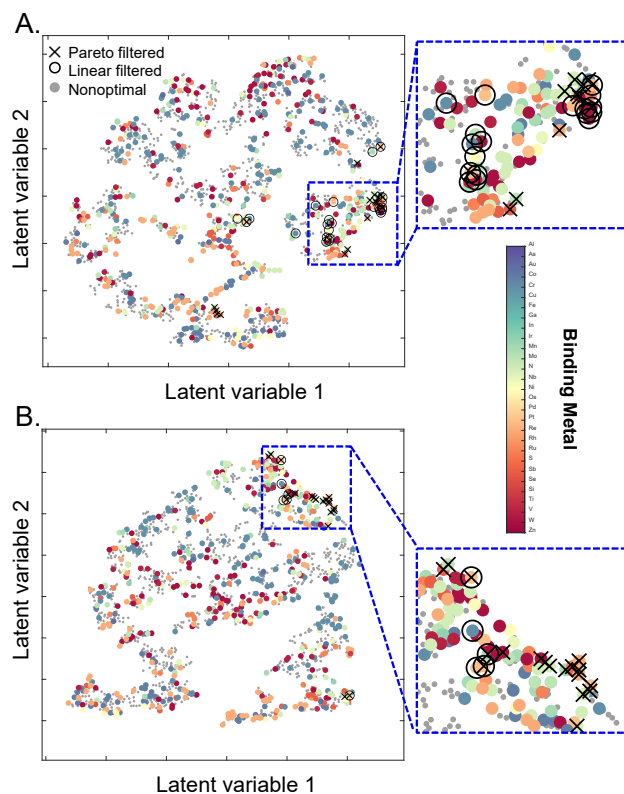


Fig. 4 Scatter plot of 1,555 surfaces for acid-stable (A) HER and (B) HOR on two-dimensional latent space using t-SNE<sup>32</sup>. The candidates based on the linear and Pareto optimal filters are marked with circle and cross symbols, respectively. Grey circles denote the non-optimal candidates. Color codes represent binding metal elements.

In summary, we evaluated multiple aspects of catalyst properties to discover active, stable, CO-tolerant, and cost-effective catalysts using *GASpy* database and Materials Project. We found 18 and 4 promising candidate materials (unique MPIDs) that satisfy all criteria, and some are cost-effective (See Supplementary Information for the full list). In particular, the electrochemical stability condition filtered out a majority of materials. This study suggests that the future *in silico* catalyst discovery should be accompanied by the stability analysis, which is nearly free of cost in terms of computation time compared to the expensive DFT calculations but could effectively reduce the number of DFT jobs. We note that this analysis applies not only to the materials already in the Materials Project database but also to new systems of interest by performing bulk optimizations and plugging the results into the

Pourbaix analysis. We expect that the stability analysis would become more critical for harsher electrochemical conditions such as oxygen reduction and water oxidation.<sup>16</sup> Finally, we compared the linear and Pareto optimal filtering, and different results between the two filtering approaches suggest the importance of the target property specification during the catalyst discovery.

## Conflicts of interest

There are no conflicts to declare.

## Acknowledgements

S.B acknowledges Richie Chen (CMU) for helpful discussions during the revision.

## Notes and references

- 1 C. Wei, R. R. Rao, J. Peng, B. Huang, I. E. Stephens, M. Risch, Z. J. Xu and Y. Shao-Horn, *Adv. Mater.*, 2019, 1806296.
- 2 Z. W. Seh, J. Kibsgaard, C. F. Dickens, I. Chorkendorff, J. K. Nørskov and T. F. Jaramillo, *Science*, 2017, **355**, eaad4998.
- 3 W. Ni, A. Krammer, C.-S. Hsu, H. M. Chen, A. Schüler and X. Hu, *Angew. Chem. Int. Ed.*, 2019, **58**, 7445–7449.
- 4 M. K. Bates, Q. Jia, N. Ramaswamy, R. J. Allen and S. Mukerjee, *J. Phys. Chem. C*, 2015, **119**, 5467–5477.
- 5 S. J. Gutić, A. S. Dobrota, M. Leetmaa, N. V. Skorodumova, S. V. Mentus and I. A. Pašti, *Phys. Chem. Chem. Phys.*, 2017, **19**, 13281–13293.
- 6 R. Bar-Ziv, O. E. Meiron and M. Bar-Sadan, *Nanoscale*, 2018, **10**, 16211–16216.
- 7 N. Marković, T. Schmidt, V. Stamenković and P. Ross, *Fuel cells*, 2001, **1**, 105–116.
- 8 H. A. Gasteiger, S. S. Kocha, B. Sompalli and F. T. Wagner, *Appl. Catal. B*, 2005, **56**, 9–35.
- 9 W. Sheng, H. A. Gasteiger and Y. Shao-Horn, *J. Electrochem. Soc.*, 2010, **157**, B1529–B1536.
- 10 J. Kibsgaard, Z. Chen, B. N. Reinecke and T. F. Jaramillo, *Nat. Mater.*, 2012, **11**, 963.
- 11 J. Greeley, T. F. Jaramillo, J. Bonde, I. Chorkendorff and J. K. Nørskov, *Nat. Mater.*, 2006, **5**, 909–913.
- 12 S. Back, A. R. Kulkarni and S. Siahrostami, *ChemCatChem*, 2018, **10**, 3034–3039.
- 13 J. Greeley, T. F. Jaramillo, J. Bonde, I. Chorkendorff and J. K. Nørskov, *Materials For Sustainable Energy: A Collection of Peer-Reviewed Research and Review Articles from Nature Publishing Group*, World Scientific, 2011, pp. 280–284.
- 14 M. E. Björketun, A. S. Bondarenko, B. L. Abrams, I. Chorkendorff and J. Rossmeisl, *Phys. Chem. Chem. Phys.*, 2010, **12**, 10536–10541.
- 15 J. Greeley and J. K. Nørskov, *Surf. Sci.*, 2007, **601**, 1590–1598.
- 16 A. Jain, Z. Wang and J. K. Nørskov, *ACS Energy Lett.*, 2019, **4**, 1410–1411.
- 17 A. Jain, S. P. Ong, G. Hautier, W. Chen, W. D. Richards, S. Dacek, S. Cholia, D. Gunter, D. Skinner, G. Ceder and K. Persson, *APL Mater.*, 2013, **1**, 011002.
- 18 K. Tran and Z. W. Ulissi, *Nat. Catal.*, 2018, **1**, 696.
- 19 J. K. Nørskov, J. Rossmeisl, A. Logadottir, L. Lindqvist, J. R. Kitchin, T. Bligaard and H. Jonsson, *J. Phys. Chem. B*, 2004, **108**, 17886–17892.
- 20 P. Lindgren, G. Kastlunger and A. A. Peterson, *ACS Catal.*, 2019, **10**, 121–128.
- 21 K. A. Persson, B. Waldwick, P. Lazic and G. Ceder, *Phys. Rev. B*, 2012, **85**, 235438.
- 22 M. E. Kreider, A. Gallo, S. Back, Y. Liu, S. Siahrostami, D. Nordlund, R. Sinclair, J. K. Nørskov, L. A. King and T. F. Jaramillo, *ACS Appl. Mater. Interfaces*, 2019, **11**, 26863–26871.
- 23 J. Baschuk and X. Li, *Int. J. Energy Res.*, 2001, **25**, 695–713.
- 24 E. Leiva, E. Santos and T. Iwasita, *J. Electroanal. Chem.*, 1986, **215**, 357–367.
- 25 A. J. Hensley, K. Ghale, C. Rieg, T. Dang, E. Anderst, F. Studt, C. T. Campbell, J.-S. McEwen and Y. Xu, *J. Phys. Chem. C*, 2017, **121**, 4937–4945.
- 26 B. Hammer, L. B. Hansen and J. K. Nørskov, *Phys. Rev. B*, 1999, **59**, 7413.
- 27 R. S. Olson and J. H. Moore, Workshop on automatic machine learning, 2016, pp. 66–74.
- 28 J. Meija, T. B. Coplen, M. Berglund, W. A. Brand, P. De Bièvre, M. Gröning, N. E. Holden, J. Irrgeher, R. D. Loss, T. Walczyk *et al.*, *Pure Appl. Chem.*, 2016, **88**, 265–291.
- 29 A. H. Larsen, J. J. Mortensen, J. Blomqvist, I. E. Castelli, R. Christensen, M. Dułak, J. Friis, M. N. Groves, B. Hammer, C. Hargus *et al.*, *J. Phys. Condens. Matter*, 2017, **29**, 273002.
- 30 C. Shi, H. A. Hansen, A. C. Lausche and J. K. Nørskov, *Phys. Chem. Chem. Phys.*, 2014, **16**, 4720–4727.
- 31 S. Back, J. Yoon, N. Tian, W. Zhong, K. Tran and Z. W. Ulissi, *J. Phys. Chem. Lett.*, 2019, **10**, 4401–4408.
- 32 L. van der Maaten, *J. Mach. Learn. Res.*, 2014, **15**, 3221–3245.